# Bright electroluminescence from single-layer organic light-emitting diodes comprising an ambipolar carrier transport layer of phenyldipyrenylphosphine oxide

Toshinori Matsushima [a] and Chihaya Adachi [a,b,*]

[a] *Core Research for Evolutional Science and Technology Program, Japan Science and Technology Agency, 1-32-12 Higashi, Shibuya, Tokyo 150-0011, Japan*

[b] *Center for Future Chemistry, Kyushu University, 744 Motooka, Nishi, Fukuoka 819-0395, Japan*

**Abstract**

We investigated the carrier transport and recombination characteristics of single-layer organic light-emitting diodes (SLOLEDs) composed of a phenyldipyrenylphosphine oxide ($POPy_2$) layer doped with orange fluorescent molecules of 2,5-bis-[{bis-(4-methoxy-phenyl)-amino}-styryl]-terephthalonitrile (BST). The SLOLEDs achieved a high external quantum efficiency of 1.6 % and a high luminance of 24,000 cd/m$^2$ at a low driving voltage of 8 V. These very good electroluminescence characteristics originate from factors that include our use of the following: (1) the ambipolar $POPy_2$ layer, which can transport balanced amounts of electrons and holes, (2) a high BST doping concentration that traps injected carriers on BST molecules, and (3) insertion of an undoped $POPy_2$ layer next to a metallic cathode to prevent exction quenching.

*Keywords:* Single-layer organic light-emitting diode; Phenyldipyrenylphosphine oxide; Ambipolar carrier transport; Electroluminescence; Exciton quenching

* *E-mail:* adachi@cstf.kyushu-u.ac.jp

## 1. Introduction

Great improvements in electron-to-photon conversion efficiency and durability of organic light-emitting diodes (OLEDs) have been achieved by using multilayer OLED structures [1-7], which are typically composed of a high-work-function indium tin oxide (ITO) anode, an organic hole-transporting layer (HTL), an emitting layer (EML) (often doped with highly fluorescent [2,5] or phosphorescent [4,6,7] molecules), an electron-transporting layer (ETL), and a low-work-function metal cathode. The operating mechanism of OLEDs involves the injection and transport of electrons and holes through the HTL and ETL and the recombination of these carriers in the EML to produce electrically excited dopant molecules [3]. Since most organic layers mainly transport either electrons or holes [1-7], it is important to construct multilayer OLEDs to balance the numbers of electrons and holes injected from electrodes and obtain a high external quantum efficiency. However, manufacturing single-layer OLEDs (SLOLEDs) is possible if an organic layer can possess both electron- and hole-transporting characteristics and, in terms of reducing the number of organic layers in OLEDs and evaporation sources in a vacuum evaporator, produces better practical OLED display and lighting applications. This means that the overall cost is less than that of manufacturing standard multilayer OLEDs.

There have been many reports on electroluminescence (EL) from SLOLEDs [8-19]. In most SLOLEDs, organic hole-transporting (HTM), emitting dopant, and electron-transporting molecules (ETM) are dispersed in an electrically and optically inert polymer binder to transport both electrons and holes through films. However, the maximum external quantum efficiencies and luminance observed in most SLOLEDs have remained low, at less than 1% and 3,000 cd/m$^2$. Moreover, the driving voltages required for most SLOLEDs (> 20 V) have been much higher than those required for conventional multilayer OLEDs (< 10 V). Such poor device performance is due to the imbalanced transport of electrons and holes in organic layers and the low carrier hopping probability between dispersed HTMs (or ETMs).

In this study, we found that a thermally deposited layer of phenyldipyrenylphosphine oxide ($POPy_2$), whose chemical structure is shown in Fig. 1(a), has excellent ambipolar carrier transport characteristics. This implies the potential of manufacturing SLOLEDs because the $POPy_2$ layer can transport balanced amounts of electrons and holes. We fabricated SLOLEDs composed of an ambipolar $POPy_2$ layer doped with orange fluorescent 2,5-bis-[{bis-(4-methoxy-phenyl)-amino}-styryl]-terephthalonitrile (BST) molecules, whose chemical structure is also shown in Fig. 1(a), and demonstrated a high external quantum efficiency of 1.6% and a high luminance of 24,000 cd/m$^2$ at a voltage of

8 V in our SLOLEDs. We attribute this excellent performance to the use of the $POPy_2$ layer, which has excellent ambipolar and rather high-speed carrier transport ability [20,21].

## 2. Experimental details

We fabricated the SLOLEDs with an ambipolar $POPy_2$ layer in the following steps. Glass substrates coated with 100-nm-thick ITO layers with a sheet resistivity of 25 Ω/sq, purchased from Sanyo Vacuum Industries Co., Ltd., were ultrasonically cleaned in detergent (Cica clean *LX*-II, Kanto Chemicals Co.)/pure water (1/10 by volume) for 10 min, and then in pure water for 10 min, acetone for 10 min, and isopropanol for 10 min. We boiled the substrates in isopropanol for 5 min, placed them in an ultraviolet-ozone treatment chamber (UV.TC.NA.003, Bioforce Nanoscience, Inc.) for 20 min, and vacuum evaporated the organic and metal layers on them. To do this, we set the substrates in a vacuum evaporator, which was evacuated using a rotary mechanical pump and a turbo molecular pump. At a background pressure of around $10^{-4}$ Pa, a 100-nm-thick BST-doped $POPy_2$ layer was thermally deposited on the cleaned ITO surface at a deposition rate of 0.3 nm/s. The doping concentration of the BST guest to $POPy_2$ host molecules was precisely controlled at either 1 or 5 mol% using two quartz crystal microbalances during $POPy_2$ deposition. To complete the devices, a 100-nm-thick MgAg cathode layer (Mg/Ag = 10/1

by weight) [1,2] was thermally deposited on the BST-doped $POPy_2$ layer at a deposition rate of 0.33 nm/s. The active area of the devices was 0.785 $mm^2$. The current density-voltage-external quantum efficiency (*J-V-*$\eta_{ext}$) characteristics of the devices were measured using a semiconductor parameter analyzer (E5250A, Agilent Technology Co.) and a calibrated silicon photodiode (1930-C, Newport Co.) at room temperature. The luminance (*L*) was calculated from $\eta_{ext}$ assuming a Lambertian emission pattern.

To depict the energy-level diagrams shown in Figs. 1(b), 2(a), and 2(b), we measured the ionization potential energies (*IP*) of the organic layers and the work functions (*WF*) of the electrodes to be *IP* = -5.9 eV for $POPy_2$, *IP* = -5.2 eV for BST, *WF* = -5.0 eV for ITO, *WF* = -3.7 eV for MgAg, and *WF* = -4.7 eV for Ag using an AC-1 ultraviolet photoelectron spectroscope (Rikenkeiki Co.). We calculated the electron affinities (*EA*) of the organic layers to be *EA* = -2.8 eV for $POPy_2$ and *EA* = -3.0 eV for BST by subtracting their optical absorption onset energies (energy gap) from the *IP* values.

**3. Results and discussion**

To understand the hole and electron transport characteristics of the $POPy_2$ layer, we fabricated hole-only and electron-only $POPy_2$ devices with device structures of glass substrate/ITO anode (100 nm)/$POPy_2$ layer (100 nm)/Ag cathode (5 nm)/Al (100 nm) (the

hole-only device) and glass substrate/MgAg anode (100 nm)/$POPy_2$ layer (100 nm)/MgAg cathode (100 nm) (the electron-only device). The energy-level diagrams of these $POPy_2$ devices are shown in Fig. 1(b). The work functions of both the ITO and Ag electrodes are close to the highest occupied molecular orbital level of $POPy_2$, and the work function of the MgAg electrodes is close to the lowest unoccupied molecular orbital level of $POPy_2$, meaning that either holes or electrons can be injected in these devices [14,17,22]. We operated these hole-only and electron-only $POPy_2$ devices in both forward and reverse bias directions. In the forward bias, the ITO and Ag electrodes in the hole-only device were wired as an anode and a cathode, respectively, and the bottom MgAg and top MgAg electrodes in the electron-only device were wired as an anode and a cathode, respectively. The *J-V* characteristics of the hole-only and electron-only $POPy_2$ devices are shown in Fig. 1(c).

We found that the forward biased hole-only and electron-only $POPy_2$ devices show the almost same *J-V* characteristics, indicating that the $POPy_2$ layer can transport balanced amounts of electrons and holes. We observed no EL from these devices at all, indicating that they have the potential for single-carrier injection and transport. Although, in most multilayer OLEDs, organic HTL, EML, and ETL are stacked to balance electrons and holes injected from electrodes, the use of the $POPy_2$ layer with the excellent ambipolar

carrier transport characteristics makes it possible to manufacture SLOLEDs.

We operated these hole-only and electron-only $POPy_2$ devices in the reverse bias direction. The result is also shown in Fig. 1(c). The current densities for the reverse biased hole-only and electron-only devices were smaller than those for the forward biased hole-only and electron-only devices. We attribute the decrease in current density in the reverse biased hole-only device to a higher hole injection barrier of 1.2 eV at the Ag/$POPy_2$ interface than a hole injection barrier of 0.9 eV at the ITO/$POPy_2$ interface. In the electron-only device, we used MgAg alloy electrodes to prevent the oxidization of Mg and to improve a sticking coefficient of Mg on organic surfaces [1]. Therefore, preparing MgAg on the $POPy_2$ film would improve a sticking coefficient of Mg on the $POPy_2$ surfaces and an electron injection efficiency at these interfaces.

We fabricated SLOLEDs in which orange fluorescent BST molecules were wholly doped in the 100-nm-thick $POPy_2$ layer at a concentration of either 1 or 5 mol% (see the energy-level diagram shown in Fig. 2(a)). The EL spectrum and the *J*-*V*, *L*-*J*, and $\eta_{ext}$-*J* characteristics of the BST-doped SLOLEDs are shown in Figs. 3(a), 4(a), 4(b), and 4(c), respectively.

We observed bright EL from the 5-mol%-BST-doped SLOLED and degraded EL characteristics from the 1-mol%-BST-doped SLOLED. The EL peaks located at 570-600 nm originate from the emission of electrically excited BST molecules doped in the $POPy_2$ layers [Fig. 3(a)]. The 5-mol%-BST-doped SLOLED achieved a maximum $L$ of 20,000 cd/m$^2$ at a breakdown current density of 1,200 mA/cm$^2$ and a maximum $\eta_{ext}$ of 1.1 % at a current density of 4 mA/cm$^2$. We attribute these very good EL characteristics to the balanced injection and transport of electrons and holes that is induced by the ambipolar $POPy_2$ layer.

Comparing the device characteristics of the 1- and 5-mol%-BST-doped SLOLEDs, we found that the maximum $L$ and $\eta_{ext}$ observed in the 5-mol%-BST-doped SLOLED were much higher than the maximum $L$ of 2,100 cd/m$^2$ and $\eta_{ext}$ of 0.07% observed in the 1-mol%-BST-doped SLOLED. We explain this difference in $\eta_{ext}$ in the following way. Injected electrons and holes from the electrodes are trapped on small energy-gap BST molecules doped in the large energy-gap $POPy_2$ layer and are directly recombined on BST molecules to generate electrically excited BST molecules. When the number of doped BST molecules that act as carrier traps in the film is small, injected carriers traverse the film without recombining, lowering $\eta_{ext}$. In contrast, a high BST-doping concentration in the $POPy_2$ film traps injected carriers on BST molecules and enhances $\eta_{ext}$. Therefore, the

$\eta_{ext}$ observed in the 5-mol%-BST-doped SLOLED was markedly higher than that of the 1-mol%-BST-doped SLOLED. A similar carrier-trapping effect has been reported in other work on SLOLEDs [13,14].

We measured the absolute photoluminescence quantum efficiency ($\eta_{PL}$) of 1- and 5-mol%-BST-doped $POPy_2$ films to be 60 ±1 and 38 ±2% using an integrating sphere system [23]. Using these $\eta_{PL}$, the theoretical limit of $\eta_{ext}$ is expressed as the equation [23],

$$\eta_{ext} = \eta_{out}\ \eta_{e/h}\ \eta_{exciton}\ \eta_{PL},$$

where $\eta_{out}$ is the light out-coupling efficiency, $\eta_{e/h}$ is the charge balance factor, and $\eta_{exciton}$ is the efficiency of the single or triplet exciton generation. By assuming $\eta_{out}$ = 20% [23], $\eta_{exciton}$ = 25% [23], and $\eta_{e/h}$ = 100%, the theoretical $\eta_{ext}$ can be calculated at approximately 3.0% for the 1-mol%-BST-doped SLOLED and 1.9% for the 5-mol%-BST-doped SLOLED using the equation. Comparing the experimental and theoretical $\eta_{ext}$, we estimated that the percentage of recombined carriers at the maximum $\eta_{ext}$ is 2% for the 1-mol%-BST-doped SLOLED and 57% for the 5-mol%-BST-doped SLOLED. From this, we conclude that using a high BST doping concentration is crucial to reducing the number of carriers traversing the film without recombination.

In the wholly BST-doped SLOLED, the carrier recombination occurs in a wide region

from near the ITO to the MgAg electrodes, because the SLOLED has no heterojunction interface, which blocks and builds up charge carriers. It is widely known that excitons generated near metallic electrodes are quenched due to interaction with the metal [17,24,25], reducing $\eta_{ext}$ in SLOLEDs. To solve the exciton quenching problem, we fabricated and tested SLOLEDs in which BST molecules were locally doped in a 30-nm-wide region of the $POPy_2$ media at a concentration of 5 mol%, and an undoped $POPy_2$ layer ranging in width from $X$ = 20 to 35 and 50 nm was inserted next to the MgAg cathode to prevent exciton quenching (see the energy-level diagram shown in Fig. 2(b)). The EL spectrum and the $J$-$V$, $L$-$J$, and $\eta_{ext}$-$J$ characteristics of the locally BST-doped SLOLEDs with various $X$s are also shown in Figs. 3(b), 4(a), 4(b), and 4(c), respectively.

We had expected that the EL spectra of the locally doped SLOLEDs would have two emission peaks arising from both BST and $POPy_2$ molecules because we doped BST molecules in the narrow 30-nm-wide region. However, contrary to our expectation, we only observed EL arising from BST molecules doped in the narrow region (see Fig. 3(b)). This finding clearly indicates direct carrier trapping and recombination on BST molecules, as mentioned above.

The maximum $\eta_{ext}$ increased from 1.2 to 1.4 and 1.6% when the $X$ was increased from

20 to 35 and 50 nm. We obtained the highest $\eta_{ext}$ of 1.6% in the locally doped SLOLED with $X$ = 50 nm. Based on this result, we conclude that (1) exciton quenching by the MgAg cathode can be suppressed by inserting the undoped $POPy_2$ layer between the BST-doped layer and the MgAg cathode and (2) exciton quenching by the MgAg cathode is more dominant than that by the ITO anode.

We observed brighter EL at low driving voltages in the locally BST-doped SLOLEDs than that in the wholly BST-doped SLOLED. The $L$ at a driving voltage of 5 V was 50 cd/m$^2$ for the SLOLED with $X$ = 20 nm, 100 cd/m$^2$ for the SLOLED with $X$ = 35 nm, and 400 cd/m$^2$ for the SLOLED with $X$ = 50 nm, which were much higher than $L$ = 6 cd/m$^2$ at 5 V observed in the wholly 5-mol%-BST-doped SLOLED. The maximum $L$ achieved 24,000 cd/m$^2$ in the locally doped SLOLED with $X$ = 50 nm. We attribute this increase in $L$ to an increase in $\eta_{ext}$ and a reduction in driving voltage caused due to the reduction in the amount of BST molecules that act as carrier traps in the $POPy_2$ layers.

## 4. Conclusion

We demonstrated efficient EL from a single-layer organic light-emitting diode (SLOLED) whose structure was glass substrate/ITO anode (100 nm)/undoped $POPy_2$ layer (20 nm)/5-mol%-BST-doped $POPy_2$ emitting layer (30 nm)/undoped $POPy_2$ layer (50

nm)/MgAg cathode (100 nm). We achieved a high external quantum efficiency of 1.6% and a high luminance of 24,000 cd/$m^2$ in the SLOLED. These very good EL characteristics originated from factors that include our use of: (1) the ambipolar $POPy_2$ layer, which can transport balanced amounts of electrons and holes, (2) a high BST doping concentration of 5 mol% that traps injected carriers on BST molecules, and (3) insertion of a 50-nm-thick undoped $POPy_2$ interlayer between the BST-doped $POPy_2$ layer and MgAg cathode to prevent exciton quenching by the MgAg cathode. Finally, we would like to emphasize that these findings will play an important role in solving the underlying mechanisms of carrier transport and recombination in OLEDs and will make manufacturing OLEDs for display and lighting applications straightforward and inexpensive.

**Acknowledgements**

The authors are grateful to Seiichiro Murase and Tsuyoshi Tominaga (*Electronic and Imaging Materials Research Laboratories, Toray Industries Incorporated*) for providing us with $POPy_2$.

**References**

[1] C. W. Tang, S. A. VanSlyke, Appl. Phys. Lett. 51 (1987) 913.

[2] C. W. Tang, S. A. VanSlyke, C. H. Chen, J. Appl. Phys. 65 (1989) 3610.

[3] C. Adachi, T. Tsutsui, S. Saito, Appl. Phys. Lett. 57 (1990) 531.

[4] M. A. Baldo, S. Lamansky, P. E. Burrows, M. E. Thompson, S. R. Forrest, Appl. Phys. Lett. 75 (1999) 4.

[5] K. Okumoto, H. Kanno, Y. Hamaa, H. Takahashi, K. Shibata, Appl. Phys. Lett. 89 (2006) 063504.

[6] D. Tanaka, H. Sasabe, Y.-J. Li, S.-J. Su, T. Takeda, J. Kido, Jpn. J. Appl. Phys. 46 (2007) L10.

[7] R. Meerheim, K. Walzer, M. Pfeiffer, K. Leo, Appl. Phys. Lett. 89 (2006) 061111.

[8] J. H. Burroughes, D. D. C. Bradlley, A. R. Brown, R. N. Marks, K. Mackay, R. H. Friend, P. L. Burns, A. B. Holmes, Nature (London) 347 (1990) 539.

[9] D. Braun, A. J. Heeger, Appl. Phys. Lett. 58 (1991) 1982.

[10] J. Kido, M. Kohda, K. Okuyama, K. Nagai, Appl. Phys. Lett. 61 (1992) 761.

[11] C.-P. Lin, T. Tsutsui, S. Saito, J. Polym. Res. 2 (1995) 133.

[12] G. E. Johnson, K. M. McGrane, M. Stolka, Pure Appl. Chem. 67 (1995) 175.

[13] M. Uchida, C. Adachi, T. Koyama, Y. Taniguchi, J. Appl. Phys. 86 (1999) 1680.

[14] B. K. Crone, I. H. Campbell, P. S. Davids, D. L. Smith, C. J. Neef, J. P. Ferraris, J.

Appl. Phys. 86 (1999) 5767.

[15] Y. D. Jin, J. P. Yang, P. L. Heremans, M. Van der Auweraer, E. Rousseau, H. J. Geise, G. Borghs, Chem. Phys. Lett. 320 (2000) 387.

[16] J. P. Yang, Y. D. Jin, P. L. Heremans, R. Hoefnagels, P. Dieltiens, F. Blockhuys, H. J. Geise, M. Van der Auweraer, G. Borghs, Chem. Phys. Lett. 325 (2000) 251.

[17] D. G. Moon, O. V. Salata, M. Etchells, P. J. Dobson, V. Christou, Synth. Metals 123 (2001) 355.

[18] D. Ma, J. M. Lupton, R. Beavington, P. L. Burn, I. D. W. Samuel, J. Phys. D: Appl. Phys. 35 (2002) 520.

[19] T.-H. Huang, J. T. Lin, L.-Y. Chen, Y.-T. Lin, C.-C. Wu, Adv. Mater. 18 (2006) 602.

[20] T. Oyamada, H. Sasabe, C. Adachi, S. Murase, T. Tominaga, C. Maeda, Appl. Phys. Lett. 86 (2005) 033503.

[21] T. Matsushima, C. Adachi, Appl. Phys. Lett. 89 (2006) 253506.

[22] I. D. Parker, J. Appl. Phys. 75 (1994) 1656.

[23] Y. Kawamura, H. Sasabe, C. Adachi, Jpn. J. Appl. Phys. 43 (2004) 7729.

[24] A. L. Burin, M. A. Ratner, J. Phys. Chem. A 104 (2000) 4704.

[25] D. E. Markov, P. W. M. Blom, Appl. Phys. Lett. 87 (2005) 233511.

**Figure captions**

Fig. 1. (a) Chemical structures of $POPy_2$ and BST molecules. (b) Energy-level diagrams of hole-only $POPy_2$ device with ITO and Ag electrodes and electron-only $POPy_2$ device with symmetric MgAg electrodes. (c) Current density-voltage characteristics of hole-only and electron-only $POPy_2$ devices, whose energy-level diagrams are shown in (b).

Fig. 2. Energy-level diagrams of (a) wholly BST-doped SLOLEDs and (b) locally BST-doped SLOLEDs with undoped $POPy_2$ layer with widths of $X$ = 20, 35, and 50 nm.

Fig. 3. EL spectra of (a) wholly BST-doped SLOLED and (b) locally BST-doped SLOLEDs with undoped $POPy_2$ layer with widths of $X$ = 20, 35, and 50 nm. These spectra were measured when SLOLEDs were operated at constant current density of 100 $mA/cm^2$.

Fig. 4. (a) Current density-voltage, (b) luminance-current density, and (c) external quantum efficiency-current density characteristics of SLOLEDs comprising ambipolar $POPy_2$ layer.

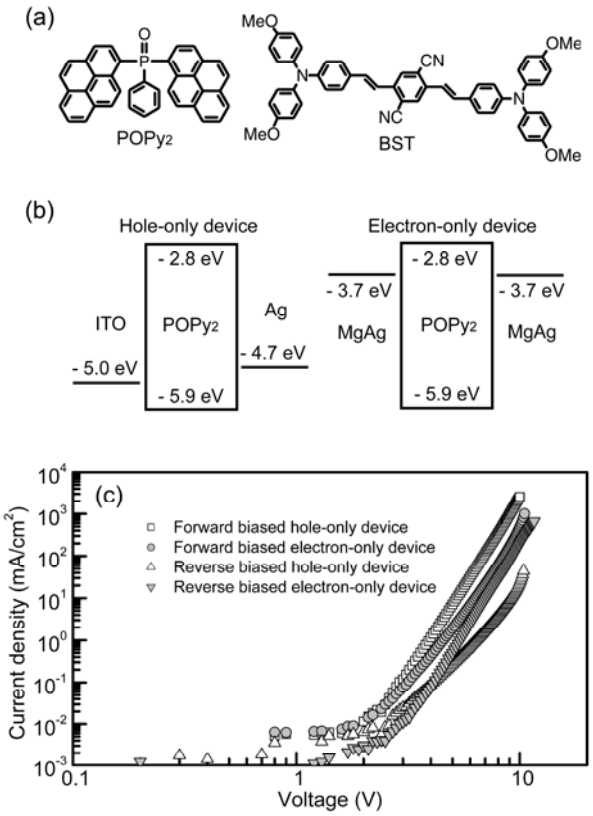


Fig. 1.

T. Matsushima and C. Adachi

Thin Solid Films

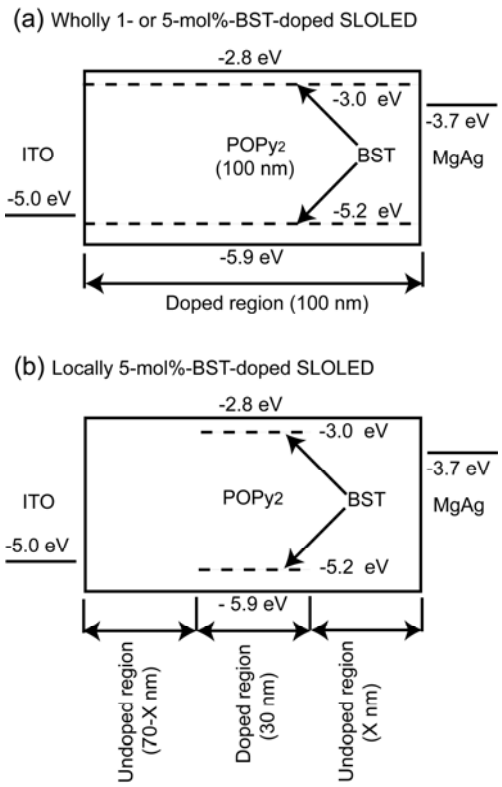


Fig. 2.

T. Matsushima and C. Adachi

Thin Solid Films

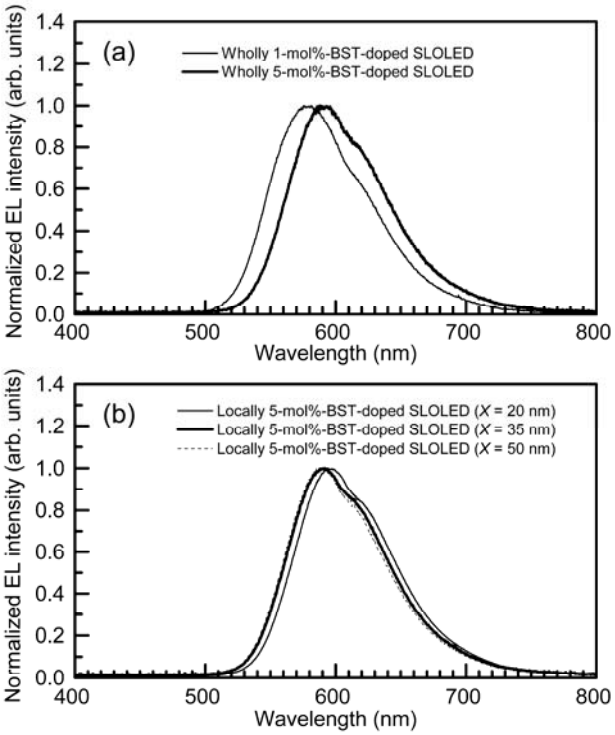


Fig. 3.

T. Matsushima and C. Adachi

Thin Solid Films

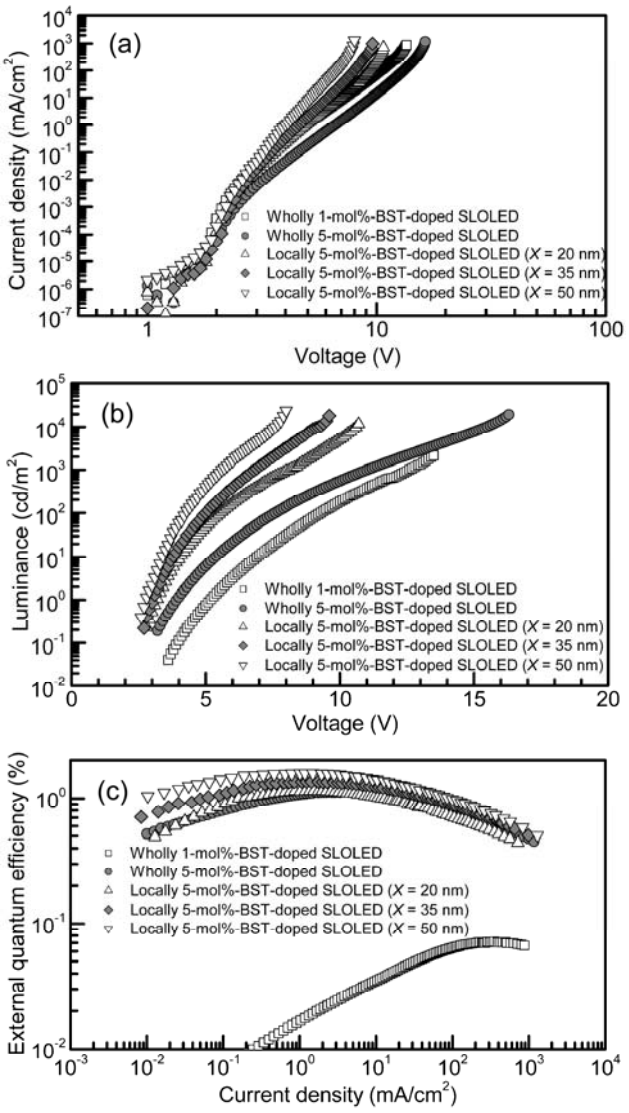


Fig. 4.

T. Matsushima and C. Adachi

Thin Solid Films